

Optimization of the array mirror for time reversal techniques used in a half-space environment

Blaine M. Harker

*Acoustics Research Group, Department of Physics and Astronomy,
Brigham Young University, N283 Eyring Science Center, Provo, Utah 84602
blaineharker@gmail.com*

Brian E. Anderson

*Geophysics Group (EES-17), Los Alamos National Laboratory, MS D446,
Los Alamos, New Mexico 87545
bea@lanl.gov*

Abstract: Time reversal (TR) utilizes an array of transducers, a time reversal mirror (TRM), to locate sources. Here TR is applied to simple sources using steady-state waveforms in a numerical, point source model in a half-space environment. It is found that TR can effectively localize a simple source broadcasting a continuous wave, depending on the angular spacing. Furthermore, the angular spacing and the aperture of the TRM are the most important parameters when creating a setup of receivers for imaging a source. This work optimizes a TRM when the source's location is known within a region of certainty.

© 2013 Acoustical Society of America

PACS numbers: 43.60.Tj, 43.60.Fg [DC]

Date Received: January 10, 2013 **Date Accepted:** March 12, 2013

1. Introduction

Acoustic source localization methods are the subject of an ongoing field of study with a broad range of applications. One such method is time reversal (TR), a simple yet powerful technique for source localization in a complex environment.¹⁻³ Fink provided general procedures and guidelines in this field,⁴ one of which is presently considered regarding proper spacing for transducers (or elements) used in the array.

The efficacy of TR is dependent on the setup of receivers used. With the addition of multiple receivers, more information can be recorded from the source, and hence the backward propagation will yield a more precise and identifiable localization of the original source. If the source is a continuous wave (CW), the localization may still be spatially focused, however requiring more transducers in contrast to the analogous setup with a time dependent wave source in a chaotic cavity.⁵ The use of multiple transducers in the TR process constitutes an array known as the time reversal mirror (TRM).⁶

TR provides advantages to alternative sound localization techniques, but, as is the case with most ray tracing or beamforming techniques, it also has its limitations. TR is simple in that it makes no assumptions about the sound source, and it does not require complex algorithms or inputs (such as computed phase delays as in the case of beamforming techniques). Furthermore, while other sound localization methods break down with an increasingly complex environment, such as with a number of reflective surfaces, the efficiency of TR actually increases without requiring increasingly challenging methods.² Here we consider a half-space environment in which TR takes advantage of the boundary reflection, whereas beamforming would be partially inhibited by the boundary reflection.

The spacing of transducers in the setup of a TR experiment is important as grating lobes may be present in the field of interest. Fink described the spacing of TRM elements as being a primary contributor to the quality of source localization.⁴ According

to Fink *et al.*, spatial separation of TRM transducers by $\lambda/2$ (where λ represents the wavelength of the broadcast signal) is necessary to avoid grating lobes (also a general guideline in array design); however, they clarify that such spacing is not necessary if the TRM is pre-focused on the source of interest.^{4,6,7} The purpose of this letter is to provide empirical guidelines to set up an effective recording of the forward propagation step in a TR experiment. In a realistic experiment, it can quickly become impractical to use half-wavelength spacing, introducing the need for a more economical and simple experimental design. We optimize the number of transducers necessary for a TR experiment given a relative knowledge of the source location (the region of certainty) and some knowledge of the source's frequency content. To this end, the efficiency and limitations of TR source localization—due to the number of TRM sensors used, the angular coverage of the TRM, frequency limitations to the setup, and an assumed region of certainty—are the matter of investigation. The incorporation of the idea of a region of certainty is not found in previous studies, but the empirical study given here allows us to determine the region of impact in the design of a TRM. This letter considers the use of TR for CW sources and may have application to the fields of nondestructive evaluation,^{8,9} underwater applications,^{10,11} seismology,^{12,13} and biomedical research¹⁴ (the citations given are for recent publications).

2. Theoretical model

The present study uses a point source broadcasting a single frequency in a half-space environment in the absence of background noise. From a theoretical study using a single frequency, further complexity can be added using superposition of single sine wave sources that could in principle synthesize a more complex source. In many experiments, a source is complex and extended; however, usage of a point source in these analyses allows a first approximation optimization of the TRM layout sensor positions without regard to a certain type of source.

The source is placed at a position $z_0 = 1.5\lambda$ above a rigid surface, thus representing a source in a half-space environment. To represent the ground reflection in the model, the source at height z_0 was reflected about the ground plane to create a virtual source at height $-z_0$ in a free space environment. The TRM elements would thus record the superposition of two sine waves, the direct signal from the source to each coplanar TRM element, and the reflected path arrival. The forward propagation wave field, $F_{fwd}(x, y, t)$, for a given wavenumber, k , in the x - y plane of the source, is

$$F_{fwd}(x, y, t) = \frac{A}{r_d} e^{j(\omega t - kr_d)} + \frac{A}{r_r} e^{j(\omega t - kr_r)}, \quad (1)$$

where A is the magnitude, j is the unit imaginary number, ω is the angular frequency, the vector r_d represents the distance from the source to the point (x, y) on the planar field and r_r is the path from the virtual source to (x, y) .

In the backward propagation step, only the information received by each TRM element, n , can be utilized, so the individual fields from the source and virtual source cannot normally be separated, thus even though we will separate the virtual source contribution and the direct source contribution in the equation representing the broadcast of the reversed signal, we did not separate them in the model. When each element transmits the reversed signal in the half-space, there will again be two paths from the element to the original source location from the direct and reflected paths in the forward step. We define $\theta_{d,n} = -kr_{d,n}$ and $\theta_{r,n} = -kr_{r,n}$ as the spatial phase information from the direct signal and reflected signal, respectively, during the forward propagation, received by the n th TRM element located at (x_n, y_n) . $A_{d,n} = A/r_{d,n}$ and $A_{r,n} = A/r_{r,n}$ are the magnitudes from the direct and reflected signals, respectively, during the forward propagation, received by the n th TRM element at (x_n, y_n) . The back propagation wave field will be a superposition of four fields at the source location, two

that interfere constructively and two that interfere destructively. The backward propagation wave field, $F_{bkwd}(x, y, t)$, in the plane of the source is

$$F_{bkwd}(x, y, t) = \sum_{n=1}^N \left[\frac{A_{d,n}}{r'_{d,n}} e^{j(\omega t - kr'_{d,n} - \theta_{d,n})} + \frac{A_{d,n}}{r'_{r,n}} e^{j(\omega t - kr'_{r,n} - \theta_{d,n})} \right. \\ \left. + \dots + \frac{A_{r,n}}{r'_{d,n}} e^{j(\omega t - kr'_{d,n} - \theta_{r,n})} + \frac{A_{r,n}}{r'_{r,n}} e^{j(\omega t - kr'_{r,n} - \theta_{r,n})} \right]. \quad (2)$$

$r'_{d,n}$ and $r'_{r,n}$ are the distances along the direct path and the reflected path, respectively, from the n th TRM element to the point (x, y) . The first term represents a backward propagation of the original direct arrival from the TRM element to point (x, y) on the plane along the direct path. The second term represents a backward propagation of the original direct arrival from the TRM element to point (x, y) on the plane along the reflected path. The third term represents a backward propagation of the original reflected arrival from the TRM element to point (x, y) on the plane along the direct path. Finally, the fourth term represents a backward propagation of the original reflected arrival from the TRM element to point (x, y) on the plane along the reflected path. It is worth noting that at the original source location $r'_{d,n} = r_{d,n}$ and $r'_{r,n} = r_{r,n}$, and the first and fourth terms' phase components reduce to $j\omega t$, thus these two terms constructively interfere to provide the TR focus. Once the individual fields for each element-source combination are calculated in the backward propagation step, they are summed together to obtain a total reconstruction wave field.

Using the simplified model described here, parameters are quickly varied, iterated and retested, allowing a parametric study of TRM design. Additionally, many of the tests were combined to utilize available RAM and run efficiently over multiple processors simultaneously. Tests were conducted on the BYU Acoustic Research Group's Kirchhoff Server, a Dell T Series Tower Server with an Intel® Xeon® E5530 with two processors for a total of 16 threads, and 48 GB of installed RAM. BYU's Mary Lou 6 (M6), a supercomputer with over 500 nodes, each node consisting of 12 Hex-core Intel Westmere processors and 24 GB of utilizable RAM, was also utilized for increased computation speeds.

To explicitly quantify the quality of localization, a metric is developed, namely the source to field ratio (*SFR*). *SFR* allows for a comparison across many parameters and their effects on the focusing quality. The *SFR* measures the pressure magnitude at the original source location and compares this to the average of the magnitude of the local field surrounding the source as

$$SFR = \frac{|F_{0,0}|}{\frac{1}{K} \sum_{m,n} |F_{m,n}|}. \quad (3)$$

$F_{m,n}$ is the pressure at a given point of the field, the source is located at the origin, and K is the number of field points within the field to be averaged. The field points are taken from $\lambda/4 \leq |x(m), y(n)| \leq 5\lambda/2$ for the case of a local field to be averaged with 5λ by 5λ sides. The field points are not taken for $|x(m), y(n)| \leq \lambda/4$ so as to not mix the focused pressure at the source location with the surrounding field. A high *SFR* suggests a strong focusing of energy, thus allowing localization. When $SFR = 1$, the implication is that the magnitude of the focus equals the average magnitude of the nearby field; the focus is therefore not distinguishable from the nearby field.

3. Results and analysis

Results will be given for the cases when the TRM layout is centered on the source; other results, not presented here, will be discussed which generalize our findings to a

source that is moved off-center of the TRM layout. The pressure magnitude of the back propagation wave field is utilized for analysis instead of the real part of the pressure. This has advantage in pointing out features of the field without regard to the $e^{j\omega t}$ time dependence.

In Fig. 1, the TR backward propagation wave fields are plotted when four different TRM layout densities are used in similar conditions while the total angular aperture (angular coverage around the source) is kept constant. In this case, a circular TRM layout of radius 12λ centered about the source spanning 2π radians is used. The region of certainty is a square with $5\lambda \times 5\lambda$ sides that is centered about the original source location. As the number of elements in the TRM increases, the field surrounding the immediate vicinity of the source location decreases in magnitude (relative to the source location), thereby increasing localization quality. As additional TRM elements are used, the area of decreased magnitude surrounding the source increases. Once this area encompasses the region of certainty, the *SFR* arrives at an asymptotic value. The *SFR* for the cases shown in Fig. 1 are Fig. 1(a) *SFR* = 3.88 for 10 elements (7.4λ between elements or 1.59 elements/radian), Fig. 1(b) *SFR* = 6.12 for 20 elements (3.8λ between elements or 3.18 elements/radian), Fig. 1(c) *SFR* = 6.34 for 30 elements (2.5λ between elements or 4.77 elements/radian), and Fig. 1(d) *SFR* = 6.34 for 152 elements ($\lambda/2$ between elements or 24.2 elements/radian).

The preceding type of analysis was carried out for many possible angular densities (number of elements per radian) to determine their effects on *SFR*. It was found that, in general, as the angular density of elements was increased, the quality of the localization increased up until it would reach an asymptotic value, irrespective of the shape of the TRM (whether the TRM was circular or square in shape)¹⁵ or the total angular coverage. Shown in Fig. 2 is the *SFR* as a function of the TRM element spacing (angular density) for circular shaped apertures. Notice that for this particular set of models, a sufficient linear density of elements to optimize the *SFR* is approximately 3.5 elements/radian. Beyond this value, additional TRM elements do not increase the *SFR* for the given region of interest. This means that the optimal element spacing is about 3.4λ for this specific circular mirror aperture of radius 12λ . An equivalent mirror with $\lambda/2$

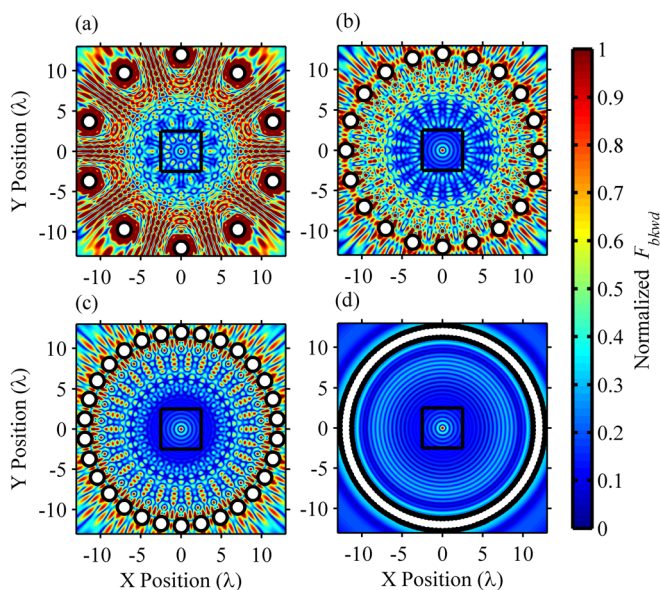


Fig. 1. (Color online) Spatial maps of the backward propagation wave fields for a 2π aperture time reversal mirror of (a) 10 elements, (b) 20 elements, (c) 30 elements, and (d) 152 elements. The backward propagation wave fields, F_{bkwd} , are normalized to the magnitude at the focal point (magnitude at the original source location).

spacing between each element would require seven times as many TRM elements. In general, for a source centered within the TRM in the aforementioned conditions, the peak value of the *SFR* would require significantly fewer TRM elements than if a half-wavelength spacing criterion was used. This peak value, and the number of TRM elements sufficient to attain it, is affected by other parameters as discussed later in this section.

The total aperture, or the angle that the TRM elements sweep out about the source, is often limited for practical purposes, and we investigate here its effects on localization. As Fink *et al.* explains, the point spread function of the source localization is related to the angular aperture of the TRM.⁶ As the angular aperture is increased, the localization becomes better resolved until the point spread function reaches the diffraction limit.²

In Fig. 2(a), a comparison of different circular-shaped TRM layouts is given with different total angular apertures, while also varying the TRM element spacing for each fixed total aperture. As an example, the cases depicted in Fig. 1, which each have a total aperture of 2π radians, can be mapped to values on the black solid line in Fig. 2(a). If the total angular aperture is increased, there is a narrowing of the point spread function near the source that yields a higher *SFR*. This increase in resolvability of the source location due to an increased aperture was noted by O'Brien *et al.*¹² and Larmat *et al.*¹³

Of particular interest is the limiting value of the *SFR* in each trial that suggests a relative independence between TRM spacing and the aperture. If the curves of Fig. 2(a) are normalized to their respective peaks, as shown in Fig. 2(b), the optimal TRM spacing for each aperture is only minimally affected. The similar trend of each aperture suggests only a minimal dependence between the actual angular spacing of the elements. As seen in Fig. 2(b), the value at which the *SFR* approaches a peak asymptotic value is essentially independent of the total aperture angle. This value is reached at about 4 elements/radian [between the results shown in Figs. 1(b) and 1(c)]. For smaller aperture sizes, the effect of beaming in the direction of the source for TRMs of smaller total aperture does not necessarily result in a maximum pressure in the region of certainty, let alone at the actual source location. Thus in the lower limit of the aperture, the quality of localization does not increase with an increase in the angular spacing [see Fig. 2(b)] because the maximum pressure of the beam—produced by an array that is nearly a line array—is not located at the original source location. We conclude that an increased total

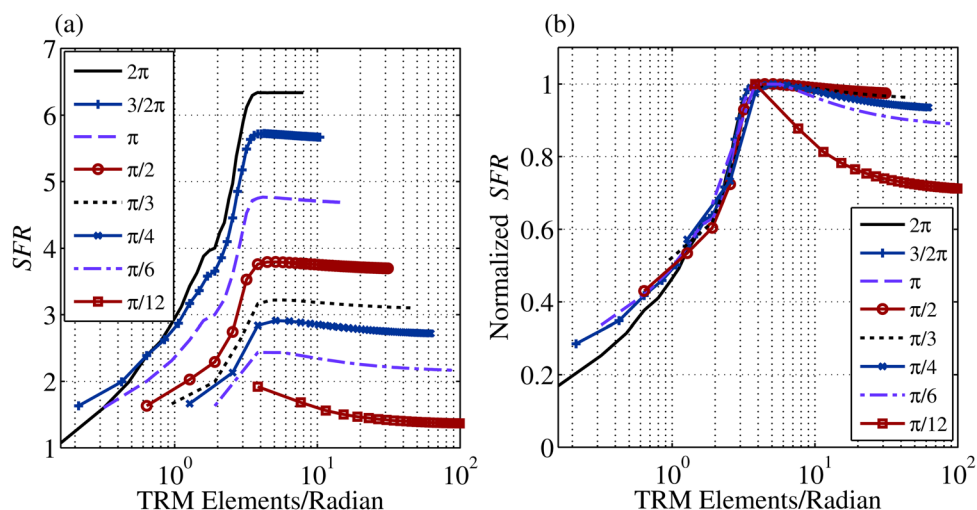


Fig. 2. (Color online) Source to field ratio versus the number of mirror elements per radian for several different total angular apertures using (a) various circular shaped time reversal mirror layouts and (b) the same data as in (a) normalized by the maximum source to field ratio of each set of data.

aperture angle, with fixed angular spacing between elements, increases the *SFR* resulting from a more optimal point spread function for the source reconstruction. Furthermore, given a region of certainty, in optimizing the peak *SFR* for each aperture, we find that there is a fixed optimal spacing irrespective of the total aperture size for the TRM. An empirical study, where the optimal angular density is extracted as the region of certainty is varied, determined the total number of elements needed given a selected total aperture (in radians, which may range from 0 to 2π), Φ , and a given region of certainty size, χ (the length of the square in wavelengths),

$$N = \frac{\Phi}{\pi}(2.1\chi - 0.65\Phi + 4.5). \quad (4)$$

This empirical relationship was determined over the range of $1\lambda \leq \chi \leq 11\lambda$ (for the results given in Figs. 1 and 2, $\chi = 5\lambda$) for the values of $\Phi = [\pi/4, \pi/2, \pi, \text{ and } 2\pi]$ and has an overall mean relative error of 8%. It has thus been found that a decreased region of certainty (better *a priori* knowledge of the source location) directly corresponds to a reduced number of elements needed in order to optimize a given TRM layout. Note that the result in Eq. (4) is based on a prefocused TRM layout and therefore has limited application.

Further studies, summarized here and discussed in detail in Ref. 15, were done using other parameters that are taken into consideration when creating a TRM setup. These include the frequency of interest, the shape and size of the TRM layout, and the degree to which the TRM is centered on the source location. Given a TRM layout and a determined optimal angular spacing of TRM elements for a respective region of certainty, if the frequency of the source is decreased, then there are more elements than necessary for optimal reconstruction. Conversely, if the frequency is increased, the TRM is no longer optimal. Thus for a certain TRM layout, there exists an upper cutoff frequency (higher frequencies would result in a decreased element spacing and naturally a decreased *SFR*), above which the TRM element spacing is not optimal. The shape of the TRM does not appear to impact the optimal angular spacing of elements nor does the distance from the TRM to the source (provided the source to be localized is not located within the near field of the TRM). Hence why the angular spacing between elements appears to be more important to specify than the actual distance between elements.

All previous results are determined for a TRM that is prefocused on the source. Cases where the source is moved off-center of the mirror were briefly considered in Ref. 15, and general findings will be highlighted here. If the source is moved off-center from the TRM, the *SFR* varies with the apparent change in the angular aperture relative to the source position. The *SFR* increases as the source is moved closer to the mirror; this corresponds to an effective increased angular aperture. However, as the source continues to approach the mirror, the quality decreases as the high amplitude in the near field of each element relative to the desired focusing greatly affects the *SFR*. If moving the source results in a decreased effective angular aperture, the *SFR* decreases.

4. Conclusions

In optimizing the layout of the TRM for a time reversal experiment, it is found empirically that for a simple source emitting a CW signal in a half-space environment, the localization quality depends on the angular density of the TRM and the region of certainty. There is a peak localization ability that, depending on the relative knowledge of the source location (region of certainty), generally allows for relaxed conditions on the half-wavelength element spacing criteria suggested by Fink *et al.*⁶ and others. Furthermore, optimization of the TRM layout is dependent on an angular density of TRM elements with respect to the source location rather than an inter-element spacing criterion. An increased total aperture, with a certain angular spacing of elements,

increases the localization ability, but it has little effect on the optimal angular spacing of elements for an assumed region of certainty. As the region of certainty decreases in area, the angular density of TRM elements necessary to reach a peak *SFR* decreases proportionally (meaning fewer elements are needed). With a better understanding regarding an optimized TRM layout, future experiments can be planned for increased efficiency. This allows for more effective use of the elements in any given experiment in any half-space application.

Acknowledgments

This research has been sponsored by the Acoustical Society of America's Robert W. Young Award and by a grant from the Office of Research and Creative Activities at Brigham Young University (BYU). We also acknowledge the BYU Acoustic Research Group as well as the Fulton Supercomputing Lab for the use of their computing resources.

References and links

- ¹A. Parvulescu and C. Clay, "Reproducibility of signal transmissions in the ocean," *Radio Elec. Eng.* **29**, 223–228 (1965).
- ²M. Fink, "Time reversed acoustics," *Phys. Today* **50**, 34–40 (1997).
- ³B. E. Anderson, M. Griffa, C. Larmat, T. J. Ulrich, and P. A. Johnson, "Time reversal," *Acoust. Today* **4**(1), 5–16 (2008).
- ⁴M. Fink, "Time-reversal of ultrasonic fields. I. Basic principles," *IEEE Trans. Ultrason. Ferroelectr. Freq. Control.* **39**(5), 555–566 (1992).
- ⁵B. E. Anderson, R. A. Guyer, T. J. Ulrich, and P. A. Johnson, "Time reversal of continuous-wave, steady-state signals in elastic media," *Appl. Phys. Lett.* **94**(11), 111908 (2009).
- ⁶M. Fink, D. Cassereau, A. Derode, C. Prada, P. Roux, and M. Tanter, "Time-reversed acoustics," *Rep. Prog. Phys.* **63**(12), 1933–1995 (2000).
- ⁷M. Fink, "Time-reversal mirrors," *J. Phys. D* **26**, 1333–1350 (1993).
- ⁸B. E. Anderson, M. Griffa, P.-Y. Le Bas, T. J. Ulrich, and P. A. Johnson, "Experimental implementation of reverse time migration for nondestructive evaluation applications," *J. Acoust. Soc. Am.* **129**(1), EL8–EL14 (2011).
- ⁹F. Ciampa and M. Meo, "Nonlinear elastic imaging using reciprocal time reversal and third order symmetry analysis," *J. Acoust. Soc. Am.* **131**(6), 4316–4323 (2012).
- ¹⁰T. Shimura, Y. Watanabe, H. Ochi, and H. C. Song, "Long-range time reversal communication in deep water: Experimental results," *J. Acoust. Soc. Am.* **132**(1), EL49–EL53 (2012).
- ¹¹F. D. Philippe, C. Prada, M. Fink, J. Garnier, and J. de Rosny, "Analysis of the time reversal operator for a scatterer undergoing small displacements," *J. Acoust. Soc. Am.* **133**(1), 94–107 (2013).
- ¹²G. S. O'Brien, I. Lokmer, L. De Barros, C. J. Bean, G. Saccorotti, J. P. Metaxian, and D. Patane, "Time reverse location of seismic long-period events recorded on Mt Etna," *Geophys. J. Int.* **184**(1), 452–462 (2011).
- ¹³C. S. Larmat, R. A. Guyer, and P. A. Johnson, "Tremor source location using time reversal: Selecting the appropriate imaging field," *Geophys. Res. Lett.* **36**, L22304, doi:10.1029/2009GL040099 (2009).
- ¹⁴J. Sadler, K. Shapoori, E. Malyarenko, F. Severin, and R. Gr. Maev, "Locating an acoustic point source scattered by a skull phantom via time reversal matched filtering," *J. Acoust. Soc. Am.* **128**(4), 1812–1822 (2010).
- ¹⁵B. M. Harker, "Theoretical evaluation of continuous-wave time reversal acoustics in a half-space environment," Honors thesis, Brigham Young University, 2012.